International Forum on Aeroelasticity and Structural Dynamics
IFASD 2017
25-28 June 2017, Como - Italy

WIND TUNNEL FLUTTER TESTS OF A U-TAIL CONFIGURATION PART 2: EXPERIMENTAL AND NUMERICAL RESULTS

Hadrien J. Mamelle [1], Gabriel Broux [1], and Eric C. Garrigues [1]

[1] Dassault Aviation
78 quai Marcel Dassault, 92552 Saint-Cloud France
hadrien.mamelle@dassault-aviation.com

Keywords: U-tail, flutter, intersecting surfaces, wind tunnel tests, experimental database, numerical correlation.

Abstract: The flutter behavior of the innovative U-tail aircraft studied by Dassault Aviation is significantly influenced by specific aerodynamic phenomena which are computationally challenging to predict. This article presents the effect of the aerodynamic interactions between the U-tail surfaces on the flutter behavior as well as the corner flow aerodynamic aspects arising in the area where the tail surfaces intersect. A fruitful wind tunnel tests campaign has been successfully conducted in ONERA S2MA pressurized wind tunnel on a half U-tail mock-up which has been heavily instrumented to gather flutter and aerodynamic data in subsonic and transonic domains. Structural, aerodynamic and flutter correlations between experimental and numerical results are presented and point out that relevant and valuable data have been recorded for numerical tools assessment. Emphasis is put on the remarkable mock-up structural behavior thanks to which excellent flutter onsets repeatability has been observed. The mock-up dynamic behavior is accurately modelled by a tuned Finite Element model which modal behavior is used to compute flutter results presented in this paper. Experimental flutter curves creation and flutter mode shape extraction from the measured data are presented and demonstrate that the targeted bending-torsion flutter mechanism has indeed been measured. These experimental and numerical results give good confidence in the suitability of this comprehensive experimental database in evaluating the validity domain of numerical tools and in calibrating aerodynamic prediction tools. In the end an industrial computational strategy to accurately compute the intersecting surfaces flutter behavior and aerodynamics should be available to study conceptual aircraft configurations like the U-tail.

1 INTRODUCTION

Dassault Aviation investigates innovative aft body configurations to design greener aircrafts such as the U-tail depicted in Figure 1.

Figure 1: Innovative U-tail configuration for engine noise shielding.

This U-tail empennage configuration constitutes an innovative noise shielding concept which aims at reducing the aircraft noise footprint during flight phases like take-offs and flyovers. In addition to the estimation of the acoustic shielding capacity, the design of a U-tail raises several challenges. One of them is to accurately predict the aerodynamic interactions between the intersecting surfaces. These interactions have a direct impact on aerodynamic fields, structural loads and flutter, and thus on the configuration performance and feasibility. Furthermore the airflow quality in the vicinity of the corner where the tail surfaces cross each other is of primary importance for aircraft performances regarding drag and handling qualities. Predicting accurately the flow field in the vicinity of the corner zone is still a challenge and enhancement of computational methods requires detailed experimental data. Hence, before envisaging such innovative configurations in a new aircraft development program, demonstration tests related to the aerodynamic and flutter characteristics are necessary in order to confirm the capability to model and, so, optimize such innovative configurations.

In view of validating numerical tools and models, a half U-Tail flutter wind tunnel model has been designed, manufactured and heavily instrumented with a substantial amount of pressure sensors and many accelerometers to gather experimental data on intersecting surfaces. The flutter model is wall-mounted in the wind tunnel as depicted in Figure 2 and consists of a fixed fuselage and a half U-tail which external shape is representative of an aircraft aft body with a scale factor of 1/8.

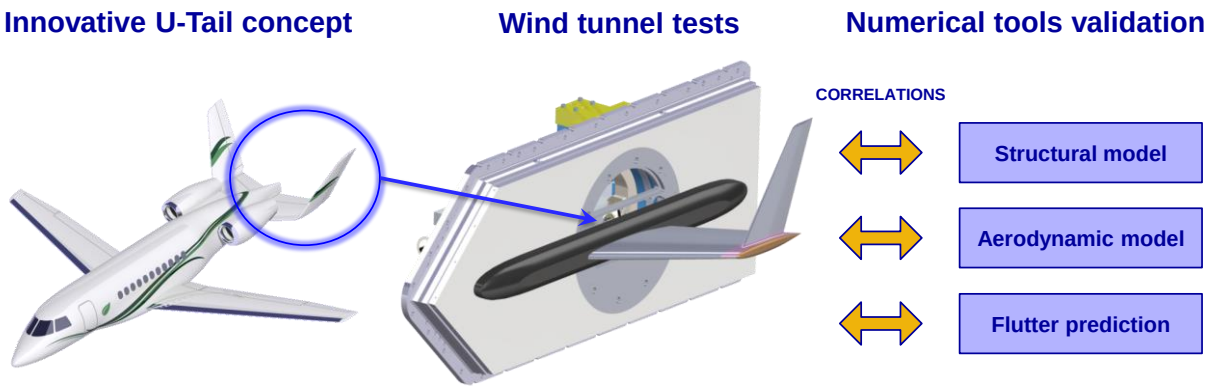

Figure 2: Wind tunnel tests of a U-tail for numerical tools validation.

As flutter is a dynamic instability resulting from the coupling between the structural dynamics and the aerodynamics, the design of this mock-up has been challenging in many respects. Several requirements on the flutter behavior have driven the mock-up architecture, in particular flutter had to occur inside the wind tunnel test range and a reliable safety system and monitoring strategy had to be set up to stop flutter onset and to ensure the structure would recover a safe and stable state. The structural behavior has been carefully analyzed in order to get a modal behavior leading to the desired bending-torsion flutter mechanism. On top of these challenges, the mock-up had to withstand high loads but also had to be modular to allow various U-tail configurations to be tested including one without dihedral and one with dihedral. The flutter model has been successfully tested in November 2016 during a wind tunnel tests campaign conducted in the pressurized ONERA S2MA facility in Modane. A comprehensive database has been acquired in subsonic and transonic domains and consists of steady and unsteady pressure field measurements as well as flutter curves measurements until flutter onset. A detailed description of the mock-up design and testing can be found in paper IFASD-2017-072 [1].

The article starts with an overview of the specific phenomena linked to U-tail configurations regarding flutter and aerodynamic aspects. In the meantime a few design aspects of the mock-up are mentioned to point out some interesting features of the mock-up structural behavior. The next part is devoted to the comparisons between experimental and numerical results. The roadmap followed to evaluate and validate the computational methodology to predict the flutter behavior of such innovative aft body configurations is presented in order to give a detailed insight of the post-processing work. Different types of experimental and numerical correlations are presented as announced in Figure 2. Structural correlations demonstrate the excellent dynamic behavior of the mock-up as well as the high level of confidence reached on the Finite Element Model (FEM). Some preliminary aerodynamic correlations are presented and give an insight about the quality of the measured data. As flutter data are unusual and rare, some data processing aspects are described to explain how to retrieve useful experimental data from acquired raw data. Good experimental and numerical flutter curves comparisons indicate that the measured flutter behavior corresponds to the targeted one. These correlations demonstrate that a fruitful wind tunnel tests campaign has been performed yielding valuable measured data in subsonic and transonic domains. The experimental database will be used to calibrate and validate numerical tools which are useful to optimize the design of innovative aircraft configurations such as the U-tail.

2 U-TAIL FLUTTER AND AERODYNAMICS

This section explains the U-tail flutter specificities and presents numerical results to illustrate the aerodynamic phenomena arising in the study of intersecting surfaces. The design aspects related to the dynamic behavior of the mock-up are also presented.

2.1 Flutter mechanism and mock-up design

The studied flutter behavior is a flutter mechanism involving two degrees of freedom, namely the primary bending and torsion modes of the Horizontal Tail Plane (HTP). The mock-up architecture has been dictated to a wide extent by the targeted flutter mechanism. Figure 3 depicts the mock-up architecture and clarifies the role of the mechanical components driving the low frequency dynamic behavior.

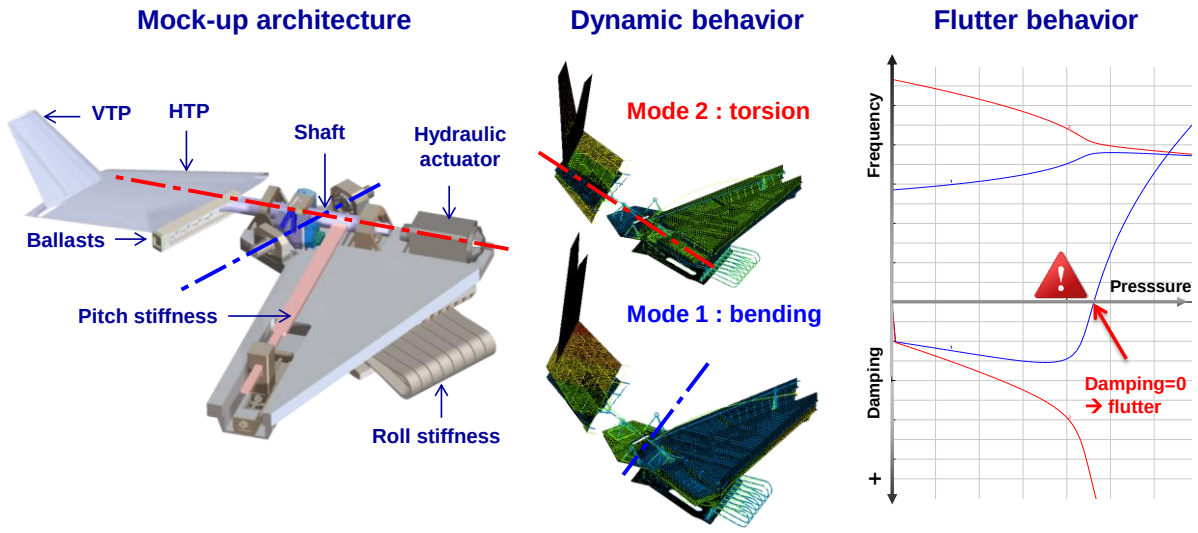

Figure 3: Mock-up architecture, dynamic behavior and flutter behavior.

The HTP is connected to a shaft which is linked to the table by two bearings and a long straight beam. This assembly ensures a pitch mode having a line of nodes through the shaft

axis (dotted red line) and which frequency is driven by the straight beam stiffness. Similarly the table is linked to the wall by two bearings and several S-shaped beams in order to get a roll mode which line of nodes lies along the wind direction (dotted blue line) and which frequency is governed by the S-Beams stiffness. The roll mode is the first HTP bending mode while the pitch mode is the first HTP torsion mode. These modes are shown in the middle of Figure 3 in which the pitch and roll axes are indicated.

Starting from this mock-up architecture which ensures the desired flutter mechanism, the mock-up design has been constrained by several requirements on the dynamic behavior. The bending and torsion modes have been isolated from the other modes in order to avoid the contribution of spurious modes in the flutter mechanism. Care was taken to ensure flutter would occur inside the wind tunnel test range by checking that flutter was sensitive to mass and stiffness variations. These variations were possible thanks to the mock-up tunability which consisted in adding ballasts and changing local stiffnesses by varying the length of the straight beam or by adjusting the number of S-Beams. Indeed both the HTP and the VTP (Vertical Tail Plane) are rigid compared to the beams leading to a great efficiency of these local stiffness variations in tuning the dynamic behavior. More details can be found on the mock-up design in paper IFASD-2017-072 [1].

2.2 Effect of aircraft configuration on flutter behavior

Flutter is governed by equation (1) which is usually expressed in a modal basis and written in the Laplace domain using the Laplace variable p. In this equation **M, C, K** are respectively the modal mass, damping and stiffness matrices, **GAF** is the generalized aerodynamic force matrix, $\mathrm{q_{dyn}}$ is the dynamic pressure, M is the Mach number, k is the reduced frequency, and X is the modal coordinate vector. The structural damping is assumed to be diagonal, thus **M, C** and **K** are diagonal matrices in opposite to the full **GAF** matrix which is the coupling matrix.

$$\left[p^2 \cdot \mathbf{M} + \mathrm{p} \cdot \mathbf{C} + \mathbf{K} - \mathrm{q_{dyn}} \cdot \mathbf{GAF}(M,k)\right] \cdot \mathrm{X}(p) = 0 \qquad (1)$$

The flutter equation can be solved, for example, by means of the p-k method from which the flutter curves can be plotted for a given Mach number as shown in the right part of Figure 3. These curves represent the frequency variations (top) and the damping variations (bottom) of the aeroelastic mock-up modal behavior with respect to an aerodynamic parameter which is here the total pressure inside the wind tunnel. Only the bending mode (blue curves) and the torsion mode (red curves) are plotted since the mock-up flutter behavior is a bending-torsion mechanism. As the pressure increases, the frequencies of these modes in the wind are constantly converging and the damping curves indicate that one mode is continuously damped (red) while the other mode damping variations depend on the total pressure (blue). As a stable (resp. unstable) state is characterized by a positive (resp. negative) damping, it appears that the mock-up becomes unstable once a critical pressure is exceeded. This unstable state is called flutter and occurs when a mode is no longer damped (blue damping equals 0 here). Flutter is characterized by an aerodynamic parameter value (critical pressure here), a frequency and a mode shape for the studied Mach number.

The comparison of the flutter behavior of two aircraft configurations like the cross tail and the U-tail depicted in Figure 4 would be meaningless since each aircraft has its own dynamic behavior, which mathematically speaking means that each aircraft is an **M – K – C** triplet. However physical insights can be gained about the effect of aircraft configuration on flutter behavior by comparing the diagrams of an HTP bending mode on these tail configurations.

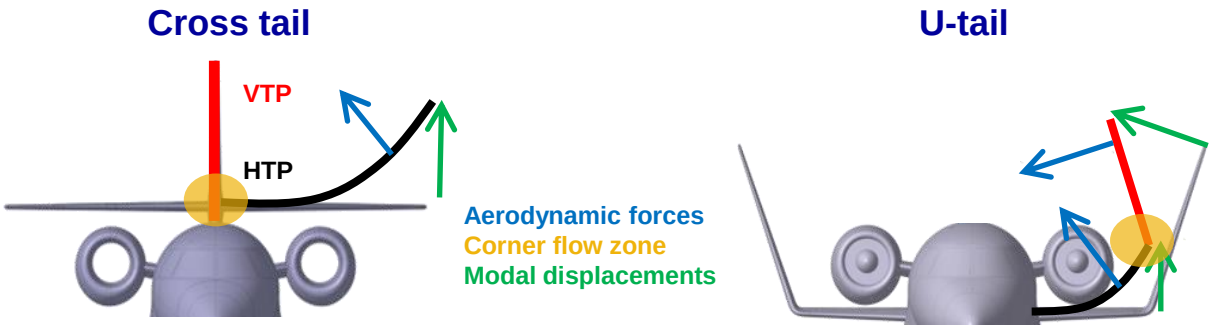

Figure 4: Cross tail aircraft (left) and innovative U-tail aircraft (right).

In Figure 4 the HTP bending mode is schematically represented by a black curve while the rigid VTP is colored in red. It appears that the VTP does not move on a cross tail whereas it follows the HTP tip displacements on a U-tail. Recalling that the modal aerodynamic work is the product of the modal displacements (green arrows) times the aerodynamic forces (blue arrows), it can be intuited that the contributions producing this work originate from very different sources between these two configurations. An obvious dissimilarity comes from the fact that the VTP creates an additional work contribution in the U-tail case since the VTP moves in the HTP bending mode. Additionally it may be anticipated that the corner flow zone (orange zone) might have a significant influence on the aerodynamic work in the U-tail case due fact that the corner is located at the HTP tip which deforms in this HTP bending mode. On the contrary the corner area cannot produce work in the cross tail case since the HTP root does not move in this schematic representation of the HTP bending mode. As the **GAF** matrix in equation (1) represents the modal aerodynamic work, it follows that the aerodynamic phenomena involved in the computation of the GAF matrix terms are closely related to the aircraft configuration. As a consequence the flutter behavior of a U-tail aircraft is sensitive to different aerodynamic phenomena compared to the one of a cross tail aircraft. The next section pushes further ahead the analysis of the flutter behavior sensitivity to the specific aerodynamic phenomena at stakes in the flutter of intersecting surfaces.

2.3 Effect of intersecting surfaces on flutter

The effect of various aerodynamic parts influencing the U-tail flutter behavior can be isolated by performing computational studies in the framework of linear aerodynamics. Starting from the modal behavior of the mock-up, the GAF matrix can be split into three contributions as shown in equation (2). Each contribution is computed by using different assumptions on the modal displacements as depicted in Figure 5. The U-tail GAF are generated by the full mode shape and the HTP (resp. VTP) GAF represents the GAF solely generated by the HTP (resp. VTP) mode shape. The GAF interaction term can be obtained by subtracting the HTP and VTP GAFs to the U-tail GAF.

$$\mathbf{GAF}_{U-TAIL} = \mathbf{GAF}_{HTP\ only} + \mathbf{GAF}_{VTP\ only} + \mathbf{GAF}_{INTERACTION} \quad (2)$$

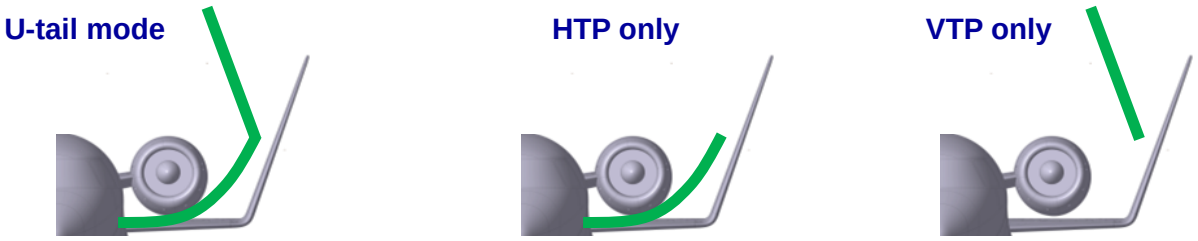

Figure 5: Modal displacement assumptions for GAF decomposition computation.

The flutter equation (1) can be solved with different GAF contributions in order to see the influence of each term on the flutter behavior. Figure 6 shows the flutter curves obtained for several GAF arrangements which are helpful to understand the effect of intersecting surfaces on the flutter behavior. The left picture indicates that the flutter behavior relies on the HTP bending and torsion mechanism since there is flutter when only the HTP GAF (blue curves) are used in the flutter equation. The flutter pressure is considerably lower when the U-tail GAF are used (red curves) which means that the VTP has somehow a destabilizing effect on the flutter behavior. This destabilizing effect can be tracked by adding the VTP GAF to the HTP GAF as done on the blue curves of the right picture. Surprisingly the VTP GAF tend to be stabilizing since the flutter pressure is higher than the one obtained using exclusively the HTP GAF. This beneficial effect stems from the fact that the VTP contribution adds damping to the torsion mode as can be noticed by comparing the damping blue curves on the left and right pictures. Finally, as the only difference between the red and blue curves on the right picture is the interaction GAF, the destabilizing effect can be entirely attributed to the aerodynamic interactions between the VTP and the HTP.

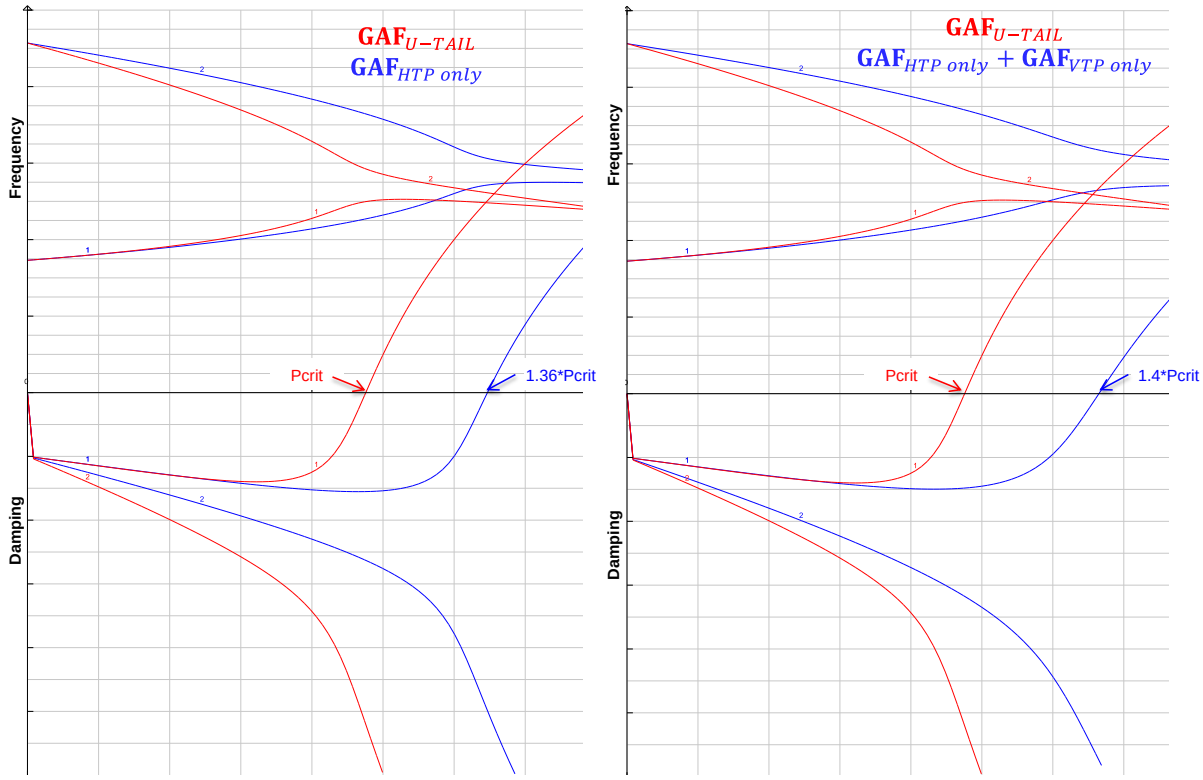

Figure 6: Effect of U-Tail on flutter (left) and effect of intersecting surface interaction (right)

This computational analysis performed in the subsonic domain highlights the fact that several GAF matrix terms participate in the overall flutter behavior of intersecting surfaces like the U-tail. These terms can have antagonistic effects and in this case the destabilizing effect of the aerodynamic interactions between the HTP and the VTP is such that flutter tends to appear sooner. Consequently flutter may become more intrusive in the structural design optimization and should be even more accurately predicted. Transonic aerodynamic phenomena add another dimension to the analysis of U-tail flutter as mentioned in the next section.

2.4 Intersecting surfaces aerodynamics

Specific aerodynamic phenomena arise in the transonic domain due to the corner located at the junction between the HTP and the VTP. Figure 7 shows the pressure field and the shape factor for different flow conditions. In the subsonic domain the flow is clean in the sense that it remains attached and subsonic over the whole surface. As the Mach number increases (from left to right), a shock wave appears in the corner area as can be seen on the pressure field picture in the middle, however the flow remains attached to the surface. Transonic flutter investigations require accurate prediction of the shock location and displacement, adding a level of complexity in the GAF computation. Finally, at even higher transonic Mach numbers, flow separation occurs in the corner area as suggested by the red color of the shape factor on the right picture. At such Mach numbers the boundary layer, the separated flow region and the shock interact with each other, leading to a challenging aerodynamic computation.

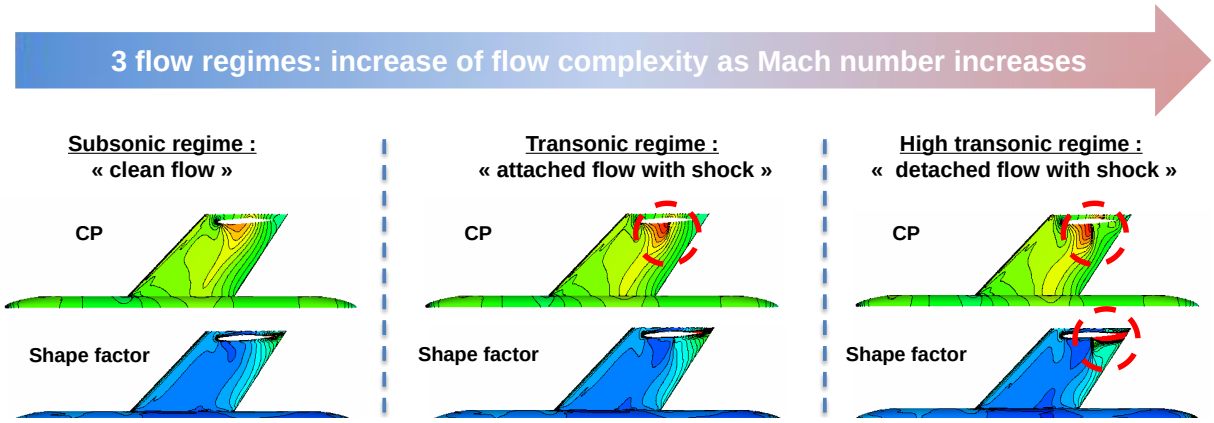

Figure 7: Intersecting surfaces flow complexity with increasing Mach number.

Aircrafts usually fly at transonic Mach numbers during flight cruise, consequently the shock location and strength should be predicted accurately for performance and handling quality issues. However detached flow conditions may come into play at these transonic Mach numbers and are to be banned to minimize the drag. These two issues both require the need for reliable numerical tools to optimize the design flight cruise. However corner flow computation is still a challenge and CFD codes should be validated before they can be used with high confidence during a new innovative aircraft development. The database acquired during the mock-up wind tunnel testing is expected to feed aerodynamicists with valuable measurements to evaluate or calibrate turbulence models and Navier-Stokes CFD codes.

Going back to flutter considerations, it is clear that these aerodynamic phenomena arising in the corner region have an influence on the GAF matrix in equation (1), therefore the flutter behavior may potentially be impacted. As already stated in §2.2, some mode shapes can have large HTP tip displacements which means that the aerodynamic pressure field in the surroundings of the corner region can create aerodynamic work. As a consequence the bending-torsion flutter mechanism might be sensitive to small variations of the pressure field in the corner zone. Once again accurate predictions are wanted in the corner flow region.

3 EXPERIMENTAL AND NUMERICAL RESULTS

This section starts with an overview of the post-processing methodology followed to assess the validity of the numerical predictions. Then structural, aerodynamic and flutter correlations between measured and computed data are presented.

3.1 Roadmap for experimental and numerical correlations

Numerical tools validation requires relevant and reliable experimental data. The measured data may be post processed in a specific way and the encountered experimental conditions must be accounted for in the computation of the numerical results. These considerations lead to a roadmap which, in the case of the present wind tunnel tests, is the one presented in Figure 8. This roadmap brings into play three main tasks (dotted black boxes) which are the structural correlation, the aerodynamic correlation and the flutter correlation. The grey boxes represent raw time data measured during the wind tunnel tests campaign. These data must be analyzed in order to extract the relevant experimental data (green boxes) that can be compared (orange arrows) to numerical results (blue boxes).

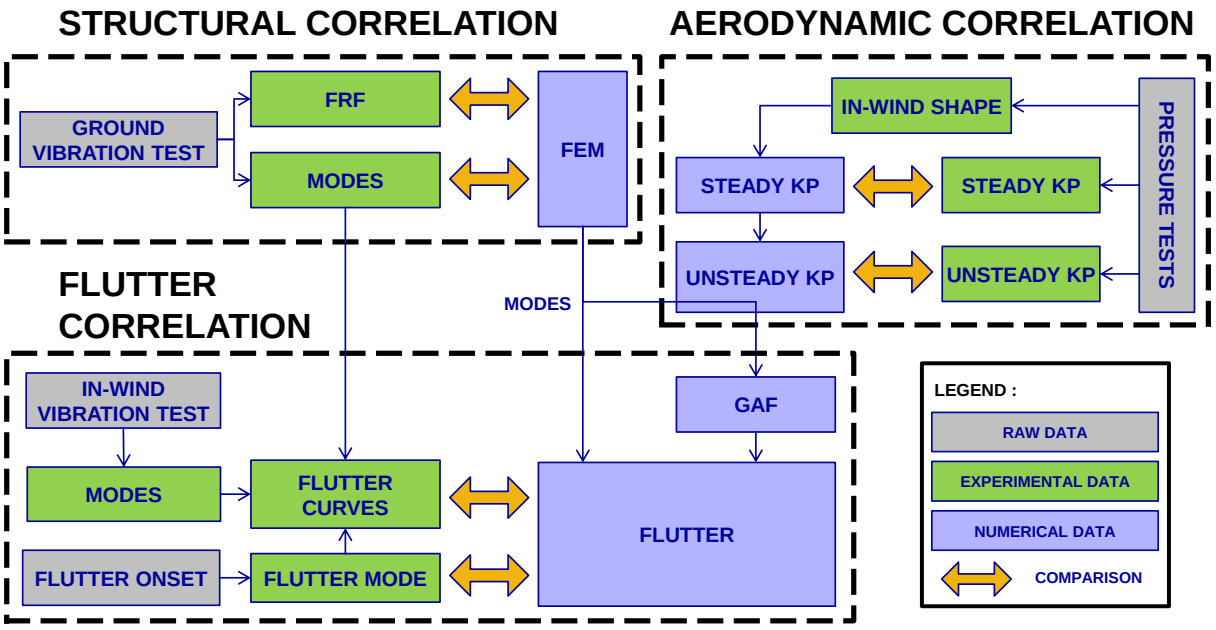

Figure 8: Roadmap for experimental and numerical correlations.

The structural correlation aims at evaluating the representativeness of the Finite Element Model (FEM). As mentioned in §2.1 the dynamic behavior of the mock-up is of paramount importance in a flutter test, therefore the dynamic behavior of the FEM should reflect as much as possible the one of the mock-up. The experimental Frequency Response Functions (FRFs) and the modal behavior of the mock-up can be measured thanks to Ground Vibrations Tests (GVT). FRFs and mode shapes comparisons between experimental and numerical are usually performed to estimate the quality of the FEM and to tune it if need be. Although the structural modeling of the mock-up is essential to numerically reproduce the measured data, it is only an intermediary step toward the aerodynamic and flutter computational tools validation.

Aerodynamic correlations include comparisons between measured and predicted steady or unsteady pressure in order to assess the accuracy of the aerodynamic models. These comparisons allow the evaluation of the validity domain of numerical models and might help to calibrate these models. Experimental steady pressure data are obtained by averaging the time data over the measurement duration while unsteady pressure data require first harmonic extraction techniques. As high subsonic and transonic Mach numbers have been investigated at high dynamic pressures, the mock-up static deformation (in-wind shape) needs to be accounted for when computing pressure fields. After a good correlation is obtained on the steady pressure field for given test conditions, unsteady pressure fields can be evaluated and compared to the measured ones.

Once a good structural model and satisfactory aerodynamic correlations are available, it is possible to move on to the flutter correlation step. The structural dynamic behavior from the FEM is used to perform the flutter computations. The modal aerodynamic work (GAF matrix) is calculated with pressure data coming either from advanced CFD methods (Navier-Stokes) or from panel methods (Doublet Lattice Method). The computation of the flutter data is then performed as explained in §2.2 and can be compared to experimental data. Experimental flutter curves and flutter mode shapes are not straightforward to retrieve from the measured raw time data, hence some post-processing steps are required to get the data of interest from the tests. In the end the objective is to validate the methodology to compute the flutter behavior of intersecting surface and to evaluate the gap between predicted and measured flutter pressure.

3.2 Structural correlation

Structural correlations between the experimental and the numerical results are presented in this section in agreement with the roadmap presented in Figure 8.

3.2.1 Mock-up dynamic behavior assessment

The structural behaviour assessment is of paramount importance when it comes to flutter testing due to the nature of the flutter phenomenon. Consequently the mock-up structural behaviour has been carefully investigated through several static tests and GVTs before going to the wind tunnel in order to ensure that the structure was linear and had the expected modal behavior. Despite several tens of flutter onsets at subsonic and transonic Mach numbers, neither structural damage nor modal behavior variation were observed, leading to very good flutter onsets repeatability.

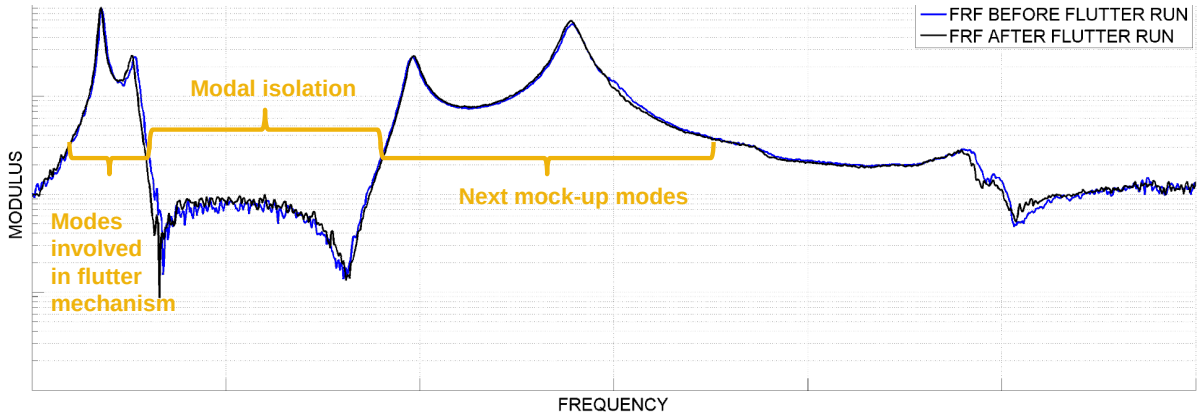

Figure 9: Measured FRF before (blue) and after (black) several flutter onsets.

GVTs were performed regularly throughout the wind tunnel tests campaign and the mock-up exhibited an excellent and repeatable structural behavior over the entire campaign. GVTs were mainly performed by exciting the mock-up with the hydraulic actuator visible in Figure 3. Two FRF measured without wind before and after several flutter tests are superimposed in Figure 9 and illustrate the good health of the structure at rest. It can also be noticed there is no spurious mode near or in between the two modes involved in the flutter mechanism which testifies that the targeted structural behaviour has been obtained. Experimental modal analysis techniques implemented in in-house tools have been used to extract the first modes of the mock-up from the GVT data. These modes have then been used to validate the FEM as presented in the next section.

3.2.2 FEM dynamic behavior validation

The FEM has been locally tuned in order to be representative of the mock-up dynamic behavior and particular care was put on the first structural modes. Comparisons between FEM results and GVT data are depicted in Figure 10. Measured (blue) and computed (red) FRFs of two accelerometers located in the VTP and on the table are superimposed and show the ability of the FEM to model the mock-up dynamic behavior of interest. The table of the cross MAC results indicates that FEM mode shapes are close to measured mode shapes, and a nearly perfect correlation is obtained for the first bending and torsion modes. These two modes are especially well simulated by the FEM which is essential as they are the ones involved in the flutter mechanism. The bending and torsion modes are depicted on the bottom left of the picture. These plots represent the normal displacements of the VTP, of the HTP and of the table, and also the VTP X displacement as indicated on the bending mode plot. It can be noticed that measured (blue) and computed (red) modal shapes agree very well explaining the correlation of nearly 100% on these modes.

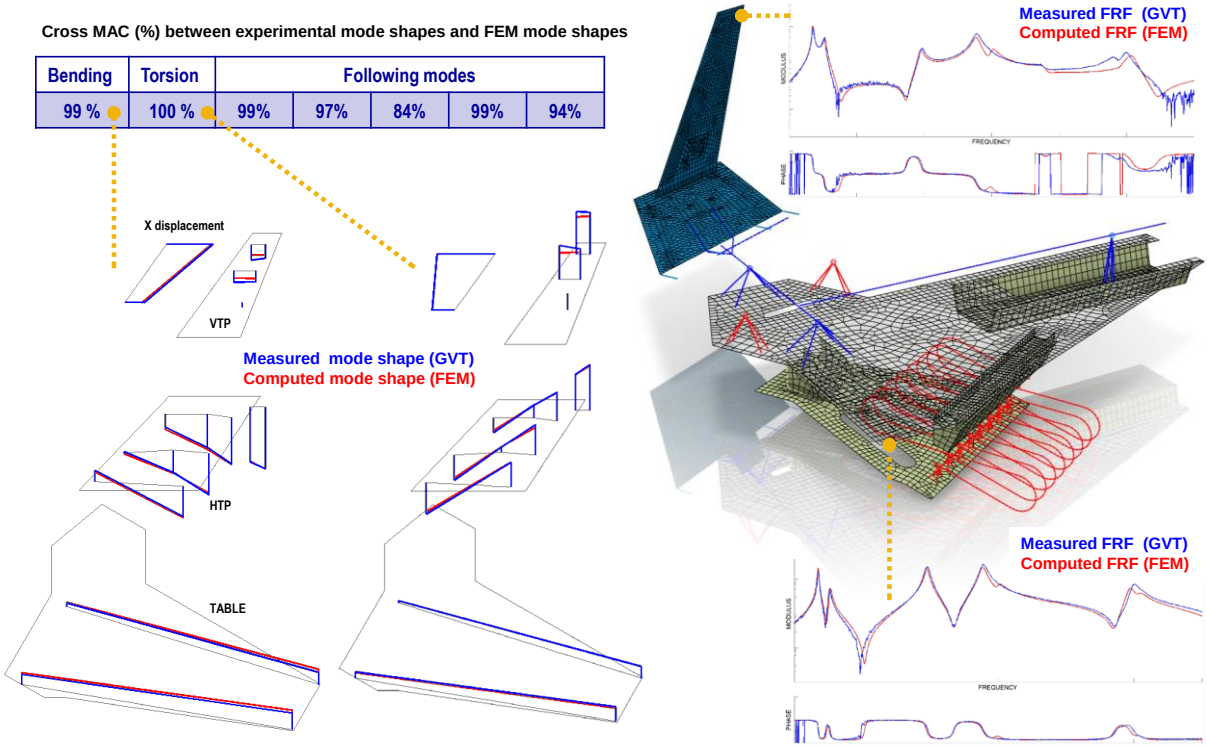

Figure 10: FRF and mode shape correlations between GVT data (blue) and FEM results (red).

The excellent correlation between the FEM results and the GVT data demonstrates not only that the mock-up has indeed a linear behavior but also that the level of details of the structural modeling is sufficient. The remarkable structural behavior of the mock-up is of great interest when it comes to correlate the numerical results with experimental data as it is only necessary to tune the FEM once for all before using the FEM modal behavior to compute the flutter corresponding to any of the numerous recorded data acquired in various configurations. It is worth mentioning that this situation is optimal in view of using the wind tunnel data to assess the aeroelastic computation process since all the effort can now focus on the data acquired with wind turned on in the wind tunnel. Furthermore, as there is no discrepancy on ground data between the FEM and the GVTs, any discrepancy on the structural behavior in the wind may be attributed to the effect of the aerodynamics on the structure.

3.3 Aerodynamic correlation

Subsonic and transonic aerodynamic data have been measured during dedicated pressure tests. Steady and unsteady pressure field measurements were acquired thanks to the hundreds of pressure sensors installed in the mock-up. During these tests pressure sensor responses have been measured while the mock-up was either maintained at a fixed steady angle of attack or excited harmonically at a fixed frequency thanks to the hydraulic actuator. Pressure coefficients (CPs) have been computed from these raw data in order to compare them with computed CPs. As shown in Figure 8 it is necessary to take into account the static deformation of the mock-up which naturally deforms due to the aerodynamic loading at such high Mach numbers. Hence 3D optical deformation measurements were used to access to the static deformation. These MDM data (Model Deformation Measurement) are available at some finite locations on the HTP and on the VTP, and have been used to reconstitute the static deformation over each surface. The resulting static deformation is applied on the CFD mesh before calculating the pressure field.

Figure 11 shows different steps needed to perform steady pressure field comparisons. Small white dots corresponding to the MDM markers can be seen on the side view picture of the mock-up. The reconstructed static shape has been applied on 2D meshes to better see the HTP (blue) and VTP (green) static deformations in the wind. Displacements of the order of magnitude of a few millimeters have been measured so the deformation has been amplified to better see the deformed static shape. Steady CPs along a VTP chord are shown on the bottom right plot in which computed CPs on the undeformed shape (red curve) and on the deformed shape (green curve) are superimposed with measured CPs (black dots). These CPs have been obtained at a transonic Mach number as evidenced by the presence of a shock. Several remarks can be deduced from this CP correlation. First the use of MDM data improves the prediction of the shock location and strength. Then the CFD code is very predictive at this transonic Mach number. Finally flow characteristics of interest like the shock location have been accurately measured thanks to the fact that sensors have been placed at appropriate locations.

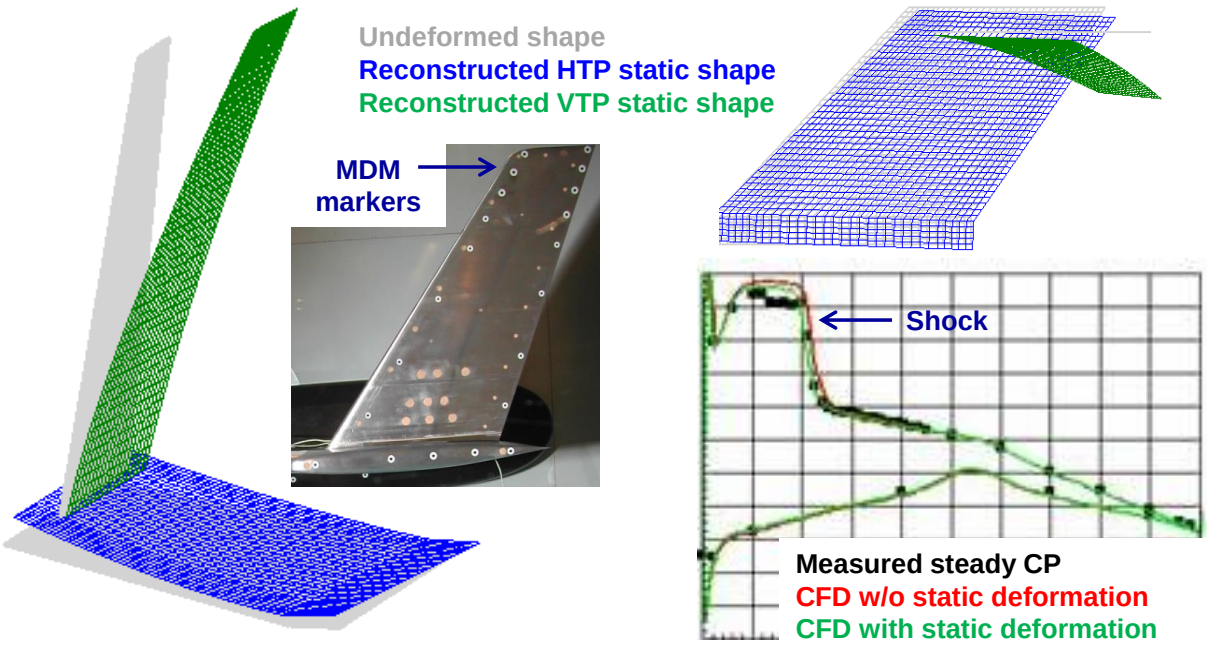

Figure 11: Effect of static deformation on steady pressure field at transonic Mach number.

3.4 Flutter correlation

This section first presents the data post processing needed to obtain experimental flutter curves and flutter mode shape. Experimental and numerical flutter results are then compared.

3.4.1 Flutter onset data processing

During flutter onset measurements the total pressure inside the wind tunnel is continually increased at fixed Mach number until flutter is observed. This sequence is illustrated in Figure 12 where the top plot is a typical time response recorded during a flutter onset measurement. Before the critical pressure, any mock-up perturbation (wind tunnel turbulence) is damped due to the fact that the structure in the wind is in a stable state (positive damping) as illustrated by the up and down arrows above the time signal. Flutter occurs right after the flutter pressure is exceeded in which case the structure vibrates at the flutter frequency on the flutter mode shape and the response amplitude grows exponentially (negative damping). Hopefully the safety system triggers when predefined thresholds are overshot and brings the mock-up back to a stable state preventing it from an impending breakdown which could also cause serious damages to the wind tunnel.

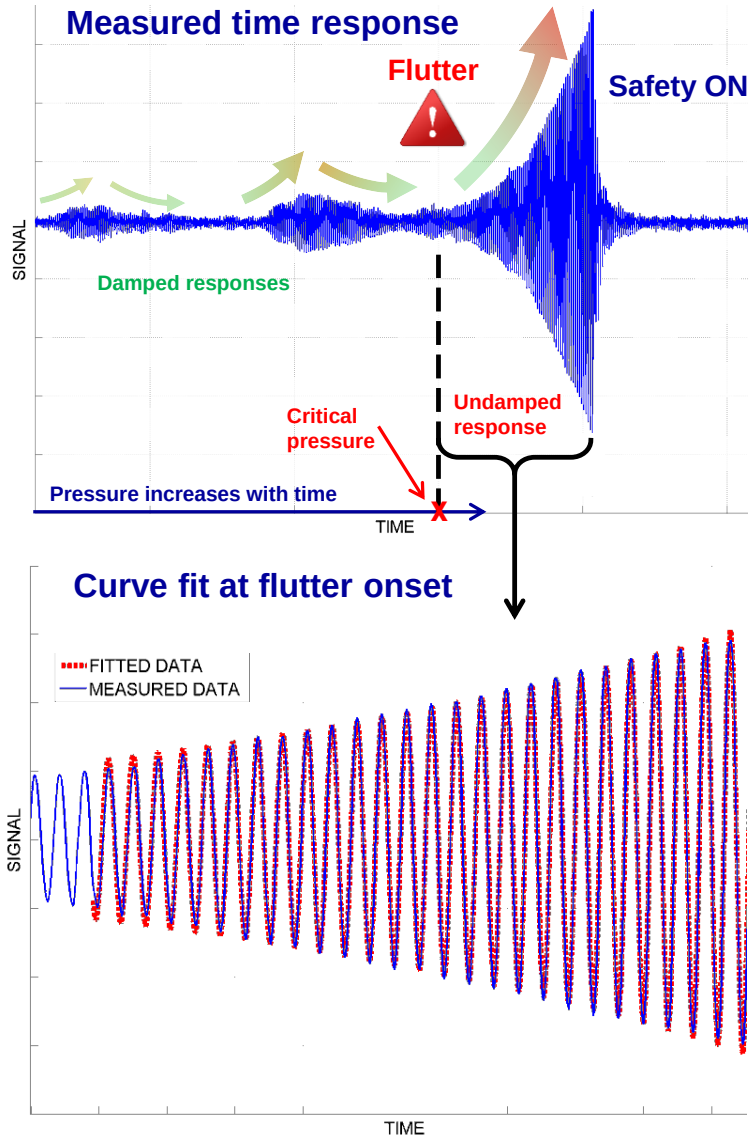

Figure 12: Time response at flutter onset (top) and data curve fitting (bottom).

Flutter onset time data require some specific data processing to get the flutter characteristics. The response at flutter onset is isolated as shown in the bottom plot of Figure 12 in order to be curve fitted with the mathematical model presented in equation (3). In this equation, A and φ are the amplitude and phase of the processed quantity when the structure experiences flutter, ω is the flutter pulsation and ξ is the flutter mode damping which is of course negative.

$$s(t) = A \cdot \mathrm{e}^{-\xi \cdot \omega \cdot \mathrm{t}} \cdot \sin(\omega \cdot \mathrm{t} + \varphi) \qquad (3)$$

The flutter frequency is obtained by applying the curve fit on any of the available time data, however the curve fit should be applied on several accelerometers time response to have access to the flutter mode shape using the A and φ obtained for each sensor. Figure 13 shows the flutter mode shape obtained by post processing the time data recorded during a flutter onset. Flutter modes are complex which is the reason why the real part (left picture) and the imaginary part (right picture) are both plotted. Going back to Figure 3 to have a look at the shaft and roll axes, it is crystal clear that the real part corresponds to a pure rotation around the shaft axis (X displacement on VTP without table displacement) whereas the imaginary part is a pure roll motion (no X displacement on VTP but table displacement). Hence the shaft motion is in quadrature with the roll motion which demonstrates that the targeted flutter mechanism has effectively been measured. This procedure can also be applied to pressure sensor time responses giving access to the aerodynamic pressure at flutter onset which could be used to check that the aeroelastic coupling is well captured by the aerodynamic numerical models.

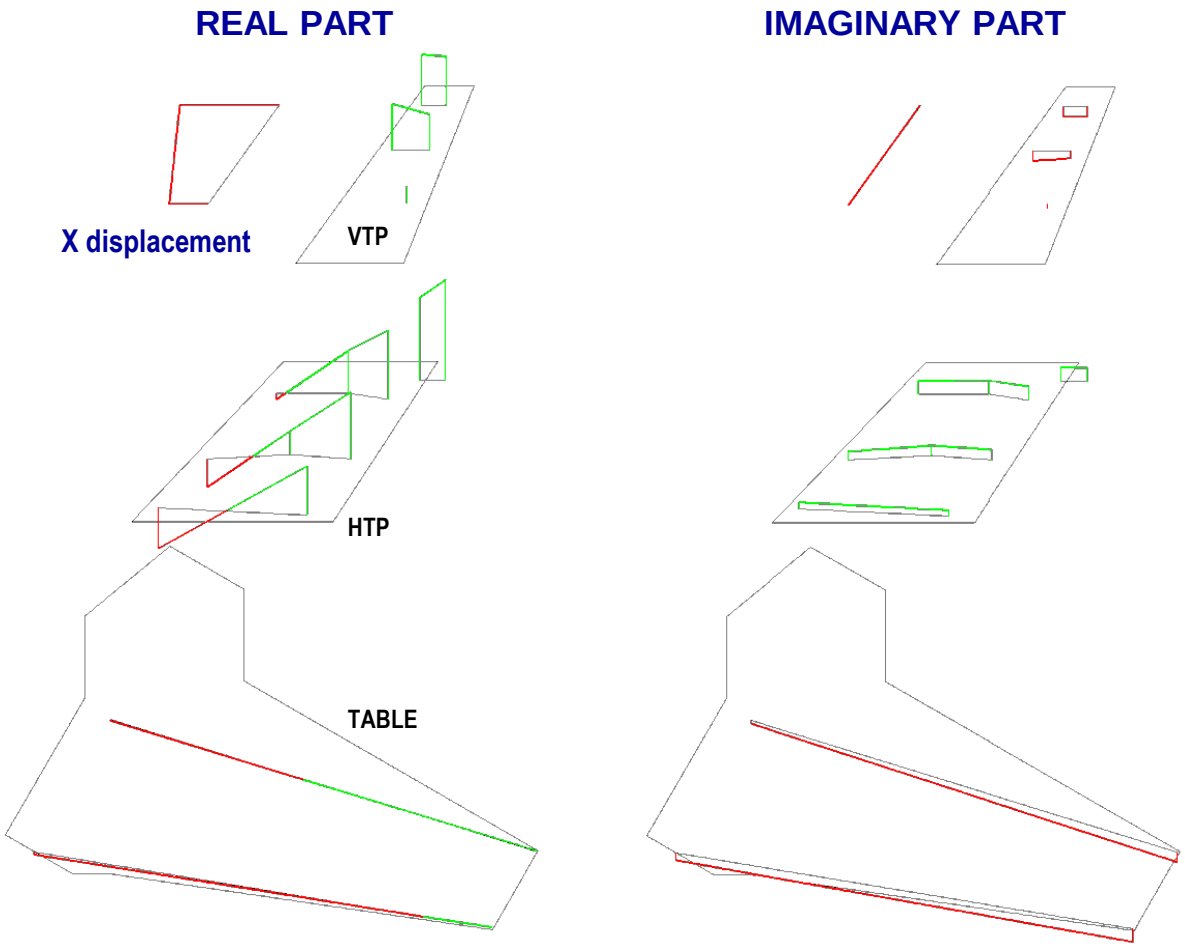

Figure 13: Flutter mode shape obtained by curve fitting of time data recorded at flutter onset.

3.4.2 Creating experimental flutter curves

Flutter curves represent the evolution of the modal frequency and damping for different flow conditions. As S2MA wind tunnel is pressurized it is possible to increase the total pressure at a fixed Mach number, therefore flutter curves can be plotted with respect to the total pressure for a given Mach number. Many measurements are needed to plot comprehensive flutter curves as the ones shown in Figure 14. A GVT must be performed to get the ground (=no-wind) modal frequency and damping of the modes of interest (left part). Then several in-wind vibration tests must be performed to discretize the flutter curves so as to see the evolution of the modal behaviour of the structure in the wind (middle part). These tests have been performed and processed in the same way GVT are with the exception that wind is turned on in the wind tunnel (§3.2.1). Finally several flutter onsets can be measured and processed as detailed in §3.4.1 to get the flutter frequency and damping which can then be added to the flutter curves (right part). Three flutter onsets have been made to build the right part of these flutter curves and it appears that flutter repeatability is outstanding. This excellent repeatability has also been noted for the other flutter onsets which have been achieved for different Mach numbers and different mock-up configurations.

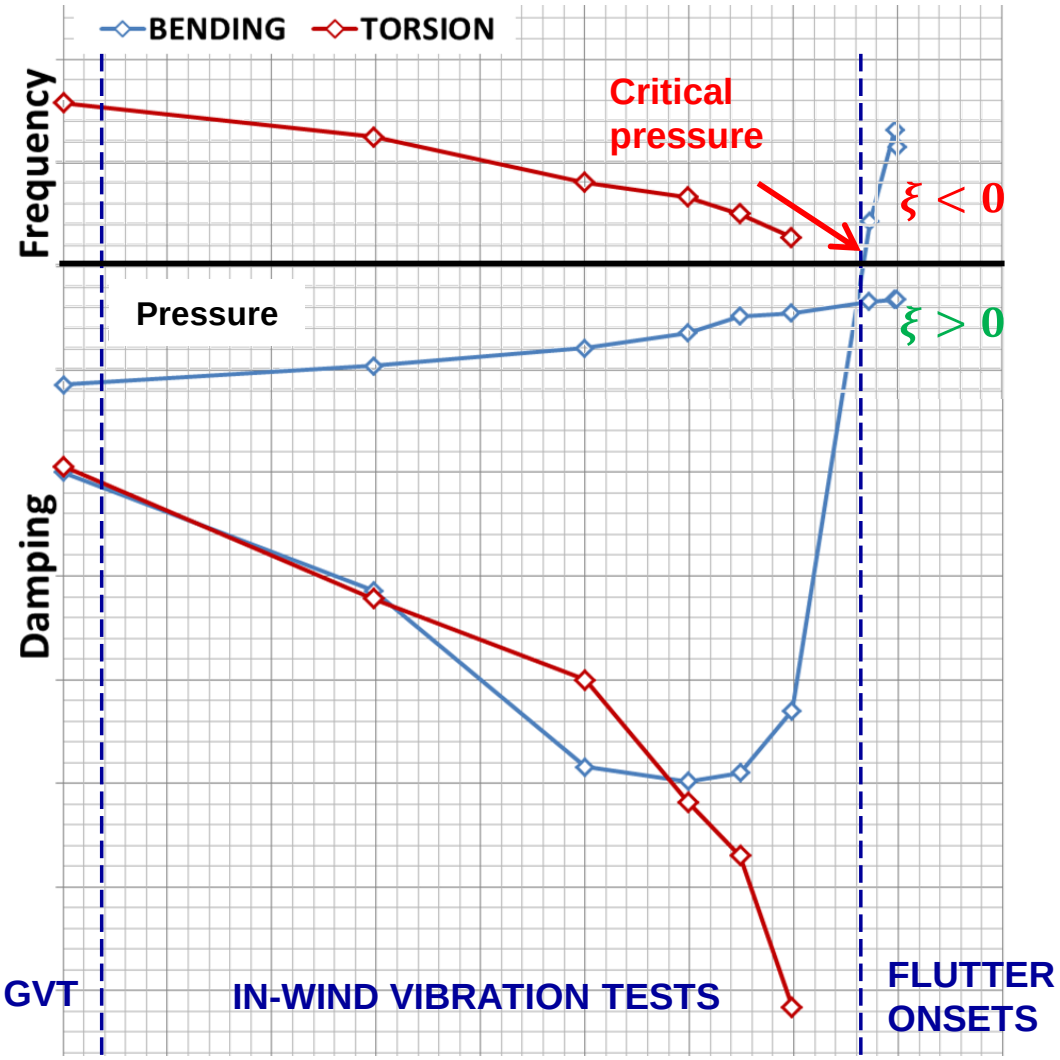

Figure 14: Data types for experimental flutter curves creation.

3.4.3 Experimental and numerical results comparisons

Based on the methodology described in the previous section, several experimental flutter curves have been built thanks to the substantial database accumulated during the wind tunnel tests campaign. Several flutter tests have been accomplished over a wide range of Mach numbers and also for several mock-up configurations to study the effect of aerodynamic phenomena (shock), geometric variations (dihedral) and stiffness variations (straight beam length) on the flutter behavior. A sample of this database is shown in Figure 15 in which the experimental (markers) and numerical (lines) flutter curves are overlaid for a Mach effect executed on a given mock-up configuration. Numerical flutter curves have been computed thanks to the tuned FEM modal behavior corresponding to the studied mock-up configuration and with GAF calculated with an in-house DLM code.

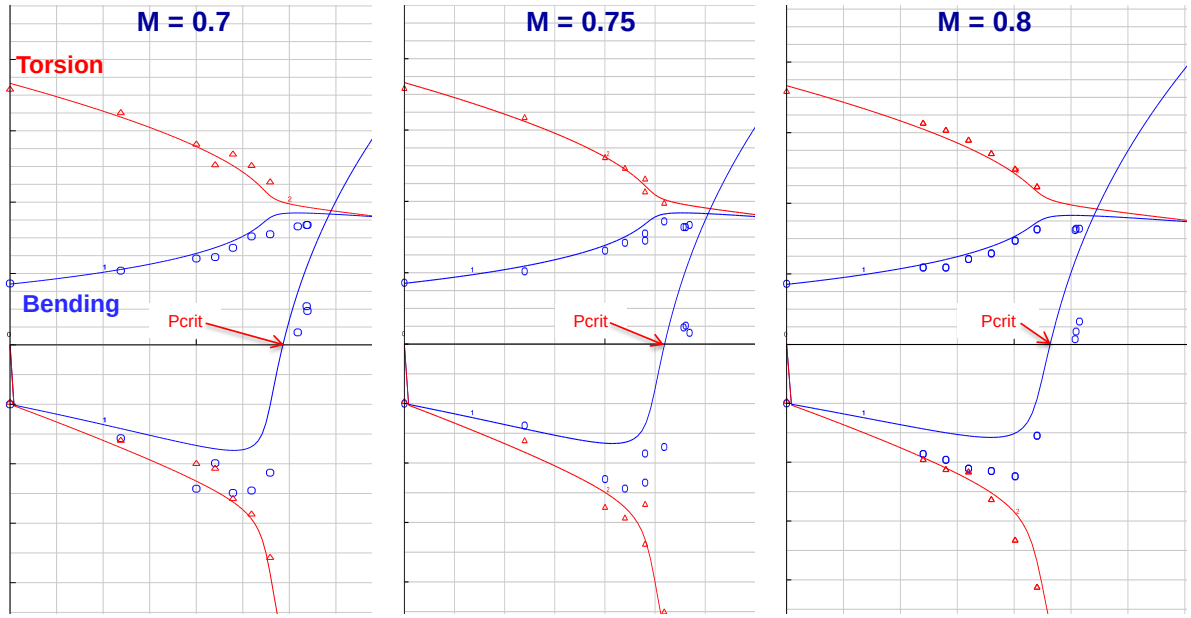

Figure 15: Experimental (markers) and numerical (lines) flutter curves for several Mach numbers.

The correlations shown in Figure 15 point out the fact the flutter prediction coincides with the measured data which testifies once again that the targeted flutter behavior has been measured during the wind tunnel test campaign. Recalling the significant effect of the aerodynamic interactions on the flutter behavior (see §2.3), it may be asserted that the aerodynamic interaction terms are reasonably well taken into account by the DLM code in this mock-up configuration, however more advanced aerodynamic checks should be performed to confirm this statement. More specifically, the frequency curves compare quite well with the experimental data. Nevertheless a slight discrepancy is observed for the highest Mach number. This may be imputed to a transonic effect that the DLM is not meant to forecast. The correlation of the damping curves is mitigated due to several details. On the one hand the measured damping might suffer from experimental uncertainties because the trends are sometimes not easy to identify. This may come from the data processing analysis or noise in the time data. On the other hand the predicted damping variations do not strictly follow the measured ones. This is especially the case for the bending mode (blue curves) which seems to be underdamped. Furthermore there is probably a transonic effect on the measured damping curves since they are quite intermixed at low Mach numbers but are separated at high Mach numbers. These matters will be further examined with CFD computations to improve the knowledge of the flutter behavior of this mock-up and thereby on the flutter behavior of intersecting surfaces.

4 FUTURE WORK AND PERSPECTIVE

The preliminary results presented in this article give good confidence in the newly recorded wind tunnel tests data since the targeted flutter behavior has been successfully attained thanks to the outstanding mock-up dynamic behavior and since the desired aerodynamic phenomena have been well captured thanks to the heavy instrumentation of the mock-up. Hence the experimental database contains valuable data over a wide range of subsonic and transonic Mach numbers and also for several geometrical and stiffness configurations which can be used for the assessment of aerodynamic codes and for the validation of the flutter computational strategy. Consequently the ongoing work will be carried on and the results presented in this article are only the premises to much more advanced numerical investigations in order to take advantage of the available experimental database.

Data processing will be applied on a wider set of measured data to have access to the full extent of the experimental database. The roadmap presented in Figure 8 will continue to be followed by introducing linearized CFD predictions (see paper IFASD-2017-050 [2]) in the comparisons with the measured data. In particular unsteady pressure data coming from the dedicated pressure tests or from flutter onset data processing will be analyzed to spot transonic effects and to estimate their influence on the flutter behavior. The aerodynamic correlation of the steady pressure field in the transonic domain is very promising and will be pursued at higher Mach number for which the detached flow issue in the corner flow region can be tackled.

The ultimate goal of this work is to define and validate an industrial strategy to predict accurately the aeroelastic stability domain of innovative aircraft configurations exhibiting intersecting surfaces like the U-tail. This objective requires to evaluate the validity domain of aerodynamic prediction tools and to increase the level of accuracy of aerodynamic phenomena prediction which may require numerical tools calibration. Precise flutter and aerodynamic computations give the ability to better optimize the aircraft design and thus to reduce weight and drag at equal or even better aircraft performance while fulfilling all the certification requirements.

5 ACKNOWLEDGEMENTS

The research leading to these results has received funding from the European Union's Seventh Framework Program (FP7/2007-2013) for the Clean Sky Joint Technology Initiative under grant agreement CSJU-GAM-SFWA-2008-001 and from the European Union's H2020 Program for the Clean Sky 2 Joint Technology Initiative under grant agreement CSJU-CS2-GAM-AIR-2014-15.

6 REFERENCES

[1] Geeraert, A. Lepage, A. Stephani, P. Feldmann, D. Häberli, W. (2017). Wind Tunnel Flutter tests of a U-Tail configuration part 1: model design and testing. *IFASD 2017 Conference Proceedings*, IFASD-2017-072.

[2] Daumas, L. Forestier, N. Bissuel, A. Broux, G. Chalot, F. Johan, Z. Mallet, M. (2017). Industrial Frequency-Domain Linearized Navier-Stokes Calculations For Aeroelastic Problems In The Transonic Flow Regime. *IFASD 2017 Conference Proceedings*, IFASD-2017-050.

COPYRIGHT STATEMENT